

Effect of Direct Extrusion on the Microstructure, Microhardness, Surface Roughness and Mechanical Characteristics of Cu-Zn-Al Shape Memory Alloy, SMA.

S. M. Al-Qawabah^{a,*}

^aTafila Technical University, Mechanical Engineering Department, Amman 11942, P.O.Box 13720, Jordan

Abstract

Shape memory alloys (SMA) are now widely used in many engineering applications especially in robotic, aerospace and vibration control area. The main problem arises from the weakness of their mechanical characteristics. Therefore, this study is directed towards enhancing the mechanical properties through severe plastic deformation. In this paper, the direct extrusion process was chosen to provide the required cold work for this purpose. A direct extrusion die was designed and manufactured to be used in this investigation for improving mechanical behavior of the Cu-Zn-Al shape memory alloy. The general microstructure, microhardness, surface roughness, and compression tests were performed on specimens from the produced Cu-Zn-Al shape memory alloy both in the as cast and after extrusion conditions. It was found that a pronounced enhancement in the mechanical characteristics of the produced Cu-Zn-Al shape memory alloy, after extrusion was achieved. The microhardness increased by 105.2 %, the flow stress was enhanced by 100 % at 0.2 strain and finally the surface roughness was reduced by 81.8 %.

© 2012 Jordan Journal of Mechanical and Industrial Engineering. All rights reserved

Keywords: Extrusion; Microstructure; Microhardness; Cu-Zn-Al shape memory alloy; Mechanical behavior; Surface roughness

1. Introduction

Shape memory alloy later referred to as SMA in this paper are alloys that can return to original shape by changing the temperature. Among a large number of SMA developed during the last two decades the Cu-based alloys serve as economic alternative to the Ti-Ni shape memory alloys due to their low cost, better electrical and thermal conductivities. The Cu-Zn-Al are now becoming the most popular Cu-based SMA. However, they suffer poor ductility problems, the martensitic stability and the intergranular crack which are disadvantageous to their application. Many attempts have been made to improve their mechanical properties and the thermal stability of the martensitic transformation [1].

1.1. Properties of shape memory alloys:

Shape recovery is due to solid-to-solid phase transformation from martensite to austenite. Austenite crystalline structure is regained upon heating, returning to its original shape [2]. SMA deforms easily under stress due to twin boundaries propagating throughout the structure in the direction of stress [6]. Fig.1 shows the details of shape memory alloy transformation

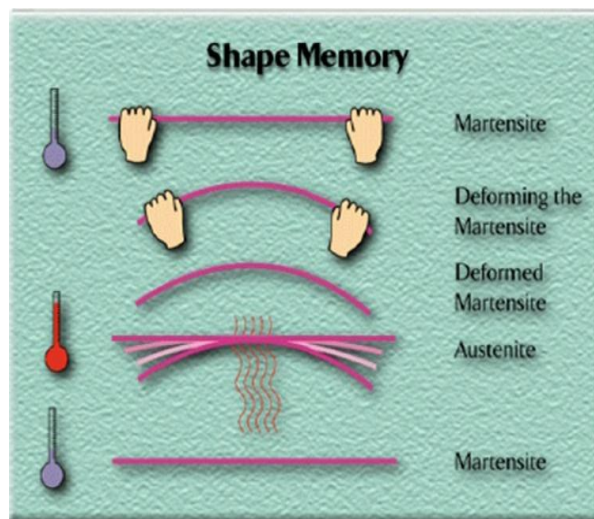


Figure 1: Shape memory alloy transformation [3].

The relationship between the applied loads and the temperature can be seen in Fig.2.

* Corresponding author. e-mail: safwan_q@yahoo.com

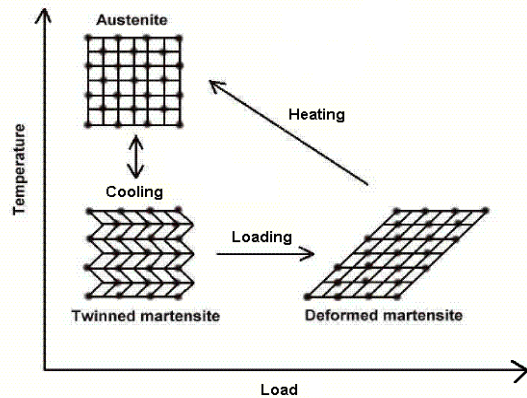


Figure 2: Load-temperature relationship of a shape memory alloy [1].

Copper-based SMA have the advantage of being made from relatively cheap materials using conventional metallurgical processes such as induction melting. Nitrogen or other inert gases should be used for shielding purposes over the melt and during pouring to prevent zinc evaporation. The handicap of these SMA is that martensitic phase is stabilized by long term aging at room temperatures. This causes an increase in transformation temperature over time [5,6]. These SMA are widely used in the engineering applications especially in the robotic, aerospace and vibration control areas. To design and optimize the applications of these alloys, a clear understanding of its behavior and characteristics is required. The phase temperatures for the shape memory alloys such as the austenite start (As), austenite finish (Af), martensite start (Ms) and martensite finish (Mf) are the basic temperatures that should be determined before designing the system. Unfortunately the properties provided by the manufacturer are normally not complete. So further investigation or testing are required.[7,8,9,10,11,12].

The main objective of this investigation is to enhance the mechanical characteristics of Cu-Zn-Al shape memory alloy.

2. Materials, Equipment and Experimental Procedures

2.1. Materials:

Mixing of three powder materials namely; pure copper, pure Zinc, and pure aluminum in appropriate percentages are normally used to prepare the Cu-Zn-Al SMA. Its chemical composition by weight is shown in Table 1.

Table 1: Chemical composition by weight of Cu-Zn-Al shape memory alloy.

Material	Cu	Zn	Al
wt. %	70 %	26 %	4%

2.2. Experimental procedures:

2.2.1. Preparation Cu-Zn-Al shape memory alloy:

The Cu-Zn-Al SMA was prepared by melting the precalculated amount of high purity copper powder at 1250 °C, then the pre-calculated amounts of pure Al and pure Zn were added to the melt in a graphite crucible. The melt was steered for 2 minutes then poured to solidify in steel mold, and cooled in air. The Cu-Zn-Al shape memory alloy was synthesized in the form of 14 mm diameter and 70 mm length cylindrical rods using melting and casting technique.

2.2.1.1. Recommended procedure to produce the Cu-Zn-Al shape memory alloy [1]:

To produce the shape memory alloy the following procedures as reported in [1] was adopted in the following sequence.

- Heating the cast (Cu- Zn- Al) to 820 °C for 10 min.
- Quenching the cast material by oil at 120 °C for 5 min.
- Cooling the cast in water at room temperature.

2.2.2. Metallurgical examination:

In this test the general microstructures Cu-Zn-Al SMA in the as cast and after extrusion condition were determined by mounting a specimen of each condition in bakelite, ground, polished and etched using enchant made of 1.5% gm powder Fe Cl₃, 96.5% wt., CH₃COOH and 2% wt. HNO₃ by weight. Photomicrographs were obtained using the NIKON 108 type microscope at magnification of 500x.

2.2.3. Determination of average grain size:

Line intercept method was used in determining the average grain size using digital microhardness tester (model HWDM-3) at 400x magnification.

2.2.4. Microhardness tests:

Microhardness measurements were taken on the surface of the polished specimens both in the as cast and after extrusion conditions at magnification 400x using HWDM-3 AT 300 gm load. Five microhardness readings were taken on the surface of each specimen from which the average microhardness was obtained.

2.2.5. Compression tests:

Cylindrical specimens of 10 mm diameter and 10 mm length of aspect ratio =1 were machined using Boxford CNC lathe machine at the same cutting conditions [depth of cut, spindle speed, feed rate]. Compression test was carried out at room temperature using (Quasar 100 Universal Testing Machine of 100 KN capacity) at 1*10⁻³s⁻¹ strain rate. The load-deflection curve was obtained for each specimen, from which the true stress-true strain curve was determined. The compression test was repeated three

times for each condition, and then the average of load-deflection curve was obtained.

2.2.6. Extrusion test:

The direct extrusion test was performed using the designed and manufactured die on (Quasar 100 Universal Testing Machine of 100 KN capacity) at $1 \times 10^{-3} \text{ s}^{-1}$ strain rate as shown in the photographs of Fig.3 (a) and (b).

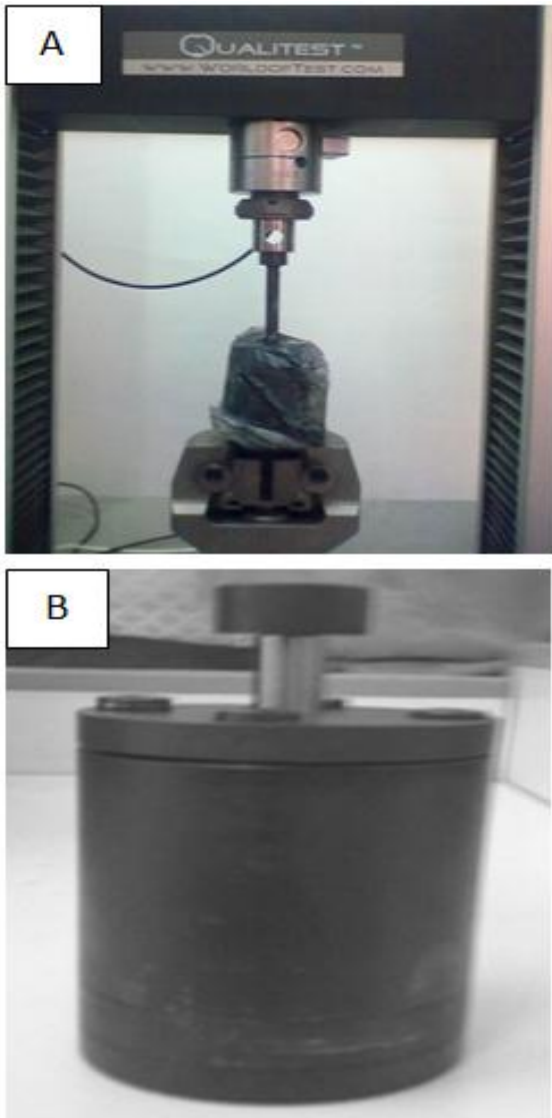


Figure 3: a) Extrusion test using instron testing machine, b) Forward extrusion die.

Fig.4 (a) and (b) shows photographs of the specimen in the as cast and after extrusion conditions. The diameter was reduced from 12 mm to 10 mm at extrusion ratio 1.44.

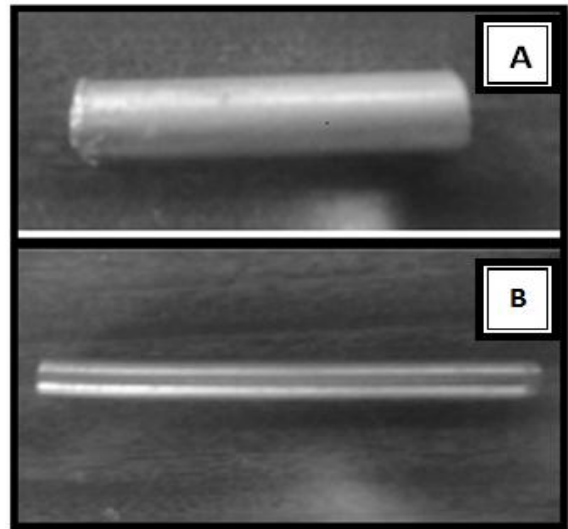


Figure 4: work part (a) as cast, (b) After extruded conditions.

3. Results and Discussion

In this section, the effect of the direct extrusion on the general microstructure, Vicker's microhardness, mechanical behavior, and surface roughness of Cu-Zn-Al shape memory alloy are presented and discussed.

3.1. Effect of Direct Extrusion on the Microstructure of Cu-Zn-Al SMA:

Figure 5 shows the general microstructure of Cu-Zn-Al SMA in the as cast condition, from which it can be seen the copper in the orange color and the Zn and Al in the dark color. The figure also indicates the uniform distribution of Zn and Al within the copper matrix. The average grain size of the Cu-Zn-Al SMA in the as cast conditions is $136 \mu\text{m}$.

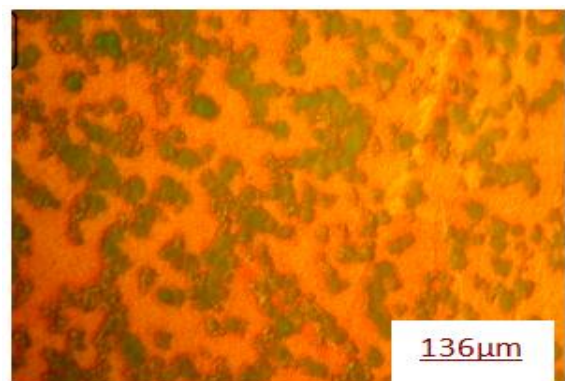


Figure 5: Photomicrograph of Cu-Zn-Al in the as cast at 200X.

The photomicrographs of Fig.6 (a-b-c-d) show the general shape of the grains in the as cast condition, which indicate an equiaxed grain type. Furthermore, It can also seen that there are square grains which indicates that the plastic deformation has occurred by twinning, Fig. 6(c).

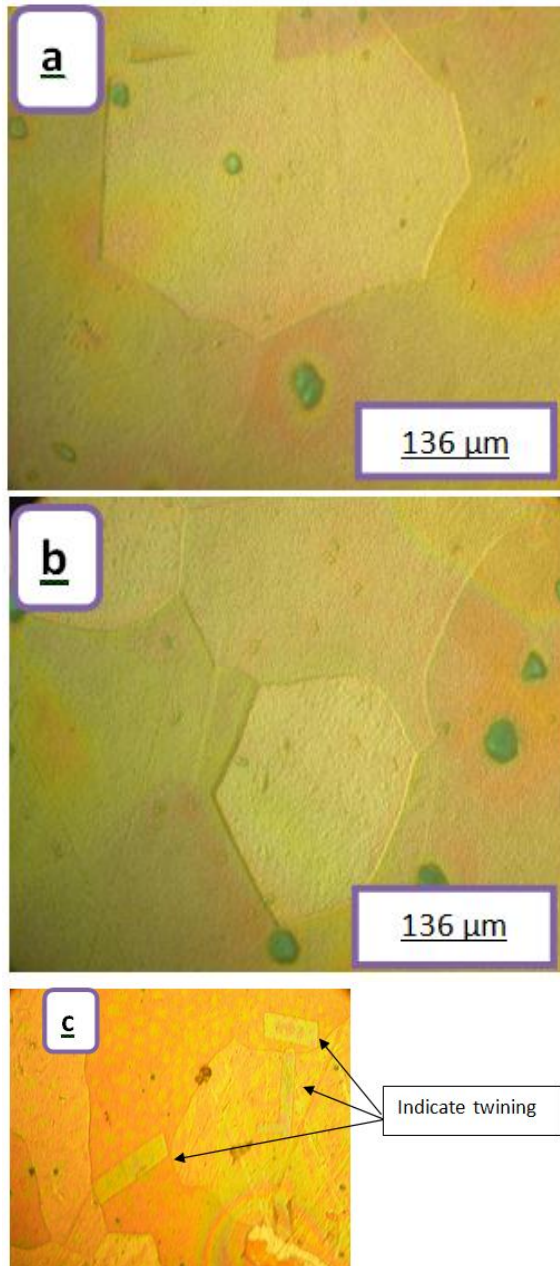


Figure 6: (a, b, c) photomicrographs showing the general microstructure of Cu-Zn-Al in the as cast condition at magnification of 500X.

Figure 7 shows the general microstructure of Cu-Zn-Al SMA after direct extrusion, from which it can be seen that the average grain size was reduced by 46.2 %. This may be explained by the enhancement in the mechanical characteristics of this alloy by the heavy plastic deformation.

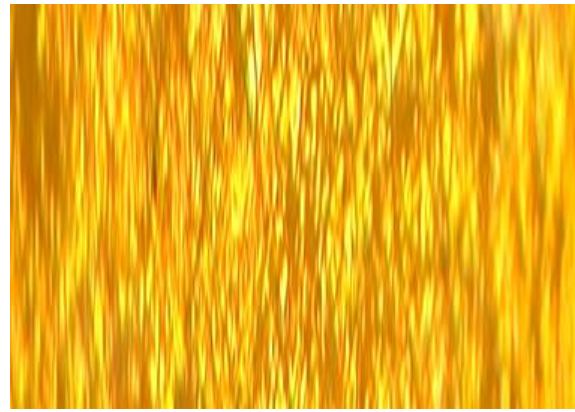


Figure 7: Photomicrograph of the microstructure Cu-Zn-Al SMA after direct extrusion, at magnification of 500X.

3.2. Effect of direct extrusion on the microhardness of Cu-Zn-Al SMA:

It is obvious from the histogram of Fig. 8 that the Vicker's microhardness of the Cu-Zn-Al SMA was greatly increased after the direct extrusion process where 105.2 % increase was achieved which is attributed to the heavy plastic deformation and the pronounced decrease in the grain size after extrusion process.

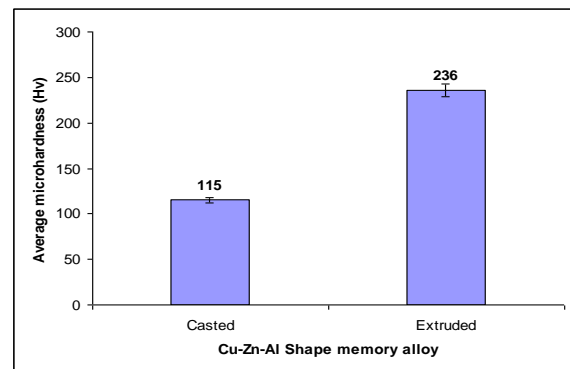


Figure 8: Average microhardness in the as cast and after extrusion conditions of Cu-Zn-Al shape memory alloy.

3.3. Effect of direct extrusion on the mechanical characteristics:

Fig.9 gives the mechanical behavior of Cu-Zn-Al SMA in the as cast and after extrusion presented by true stress-true strain curve as obtained from the autographic record of the compression test of the specimens test from the Cu-Zn-Al SMA before and after extrusion, Fig. 10(a) and (b). It can explicitly be seen from Fig.9 that the mechanical behavior is greatly enhanced by the extrusion process where about 100 % increase was achieved in the flow stress (from 200 MPa to 400 MPa). This is mainly attributed to heavy plastic deformation and the reduction in the grain size mentioned in the previous section.

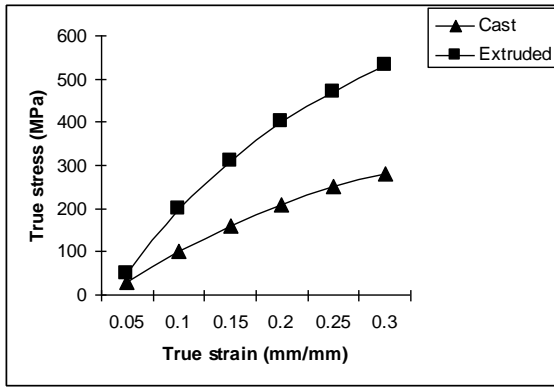
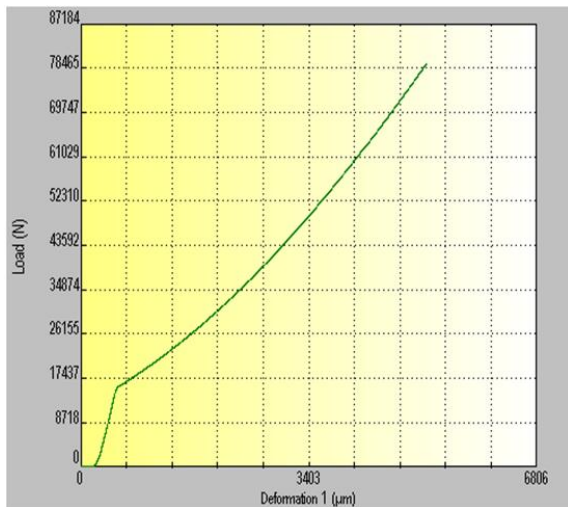
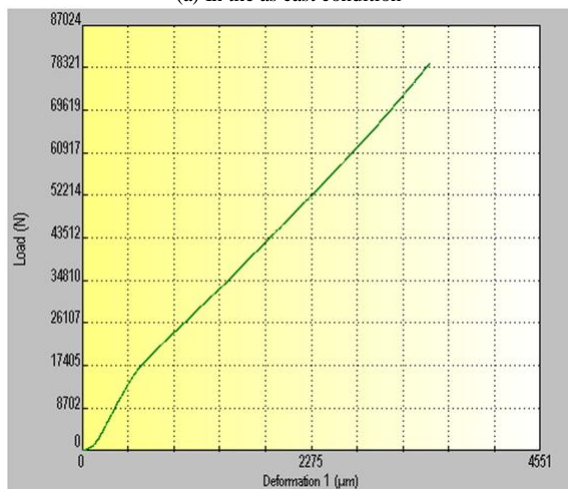


Figure 9: True stress-true strain of the as cast and after extrusion Conditions of Cu-Zn-Al shape memory alloy.



(a) In the as cast condition



(b) After extrusion

Figure 10: Autographic records (punch-displacement) for compression test on specimens (a) in the as cast condition and (b) after extrusion test.

It is also worth noting from Fig.11 that the extrusion force is 29.84 KN at the extrusion ratio 1.44 in this experimental compared to 24.54 KN, the theoretical value as obtained from theoretical analysis shown in appendix 1. The difference which is 21 % is attributed to friction and redundant forces encountered in the extrusion process.



Figure 11: Plunger (force-displacement) of Cu-Zn-Al shape memory alloy.

3.4. Effect of direct extrusion on the surface roughness of Cu-Zn-Al SMA:

It can be seen from Fig.12 that there is a pronounced enhancement in the surface quality of Cu-Zn-Al shape memory alloy after extrusion, represented by 81.8 % reduction in surface roughness, Ra, was achieved.

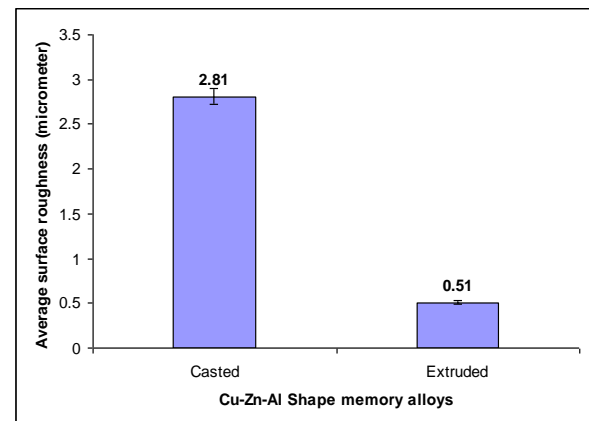


Figure 12: Average surface roughness Ra of the as cast and after extrusion Conditions of Cu-Zn-Al shape memory alloy.

4. Conclusions

The following points can be concluded:

- The average grain size of Cu-Zn-Al SMA was reduced by 46.2 % after direct extrusion process.
- There is a pronounced enhancement in the mechanical characteristics of Cu-Zn-Al shape memory alloy after forward extrusion; where the flow stress was increased by about 100 % at 0.2 strain.
- An enhancement of 105.2% was achieved in Vicker's microhardness of Cu-Zn-Al SMA after the direct extrusion process.
- The surface roughness of Cu-Zn-Al SMA was enhanced by 81.8 % after direct extrusion process.

Acknowledgment

This work has been supported by King Abdullah II Fund for Development (KAFD) and King Abdullah II Design and Development Bureau (KADDB) which are acknowledged under grant number (8/2011). Author also would like to thank Eng. Emad Yard for his help and support, author also thank students Husam Mohammad, Mohammad Zaid, and Mohamad atah for their help in the experimental work.

References

- [1] www.elsevier.com/locate/msea journal of alloys and compounds 448(2008) 331-335, Effects of Gd addition on micro structure and shape memory effect of Cu-Zn-Al alloy, available online 18 January 2007.
- [2] K. Worden, W.A. Bullough, J. Haywood "Smart technologies", World Scientific 2003, 109–135.
- [3] <http://www.talkingelectronics.com/projects/Nitinol/images> (7/6/2011).
- [4] http://webdocs.cs.ualberta.ca/~database/MEMS/sma_me_ms/sma.html ((7/6/2011).
- [5] "Shape-Memory Alloys – Metallurgical Solution Looking for a Problem", Metallurgia, Vol. 51, No. 1, January 1984, 26–29.
- [6] D. E. Hodgson "Shape Memory Applications", Inc., Wu M. H., Memory Technologies, and Biermann R. J., Harrison Alloys, Inc., <http://web.archive.org/web/20030605085042/http://www.smains.com/SMAPaper.html>.
- [7] Kiyohide Wada and Yong Liu, "Shape recovery of NiTi shape memory alloy under various pre-strain and constraint conditions". Smart Mater. Struct, Vol.14 2005, S273–S286.
- [8] Antonio Vitiello, Giuseppe Giorleo and Renata Erica Morace, "Analysis of thermomechanical behaviour of Nitinol wires with high strain rates". Smart Mater. Struct. Vol.14, 2005, 215–221.
- [9] Z.G. Wang, X.T. Zu, X.D. Feng, L.B. Lin, S. Zhu, L.P. You and, L.M. Wang, "Design of TiNi alloy two-way shape memory coil extension spring". Science and Technology of Advanced Materials, Vol. 6, 2005, 889–894.
- [10] Z.G. Wang, X.T. Zu, X.D. Feng, S. Zhu, J.W. Bao and, L.M. Wang, "Characteristics of two-way shape memory TiNi springs driven by electrical current". Materials and Design, Vol. 25, 2004, 699–703.
- [11] J. Rena, K.M. Liewa "Meshfree modelling and characterization of the mechanical behaviour of NiTi alloys". Engineering Analysis with Boundary Elements, Vol., 29, 2005, 29–40.
- [12] Mikell P. Groover. Fundamentals of modern manufacturing process and system. 3rd ed, ml, 416-430.

Appendix 1: Extrusion Calculations

In general: Force = stress * cross sectional area.

$$F_{max} = P_i * A_o \quad (1)$$

The billet dimension used is 12 mm diameter and the output diameter is 10 mm; the stress in equation (1) is the maximum of the material to be extruded.

The extrusion pressure is estimated from the Johnson equation [12].

$$P_i = Y_{extruded} (a + b \ln R) \quad (2)$$

Where;

- F_{max} : Maximum extrusion force.
 P_i : Extrusion Pressure or internal pressure.
 $Y_{extruded}$: Yield stress of the extruded material.
 R : Equal to A_o/A_f
 R : (Extrusion Ratio) = 1.44
 A_o : Initial cross-sectional area of the billet.
 A_f : Final cross-sectional area of the extruded part.
 a & b : Are constants for the material to be extruded.

$$P_i = 160 * (0.8 + 1.5 * (0.3646)) = 215.504 \text{ MPa}$$

$$F_{max} = P_i * A_o = 215.504 * \left(\frac{\pi(12)^2}{4}\right) = 215.504 * 113.097 = 24.372 \text{ kN}$$

Appendix 2: FEM Analysis

Licensed solidwork software is used in FEM investigation for punch, die, and extruded part.

1. Punch

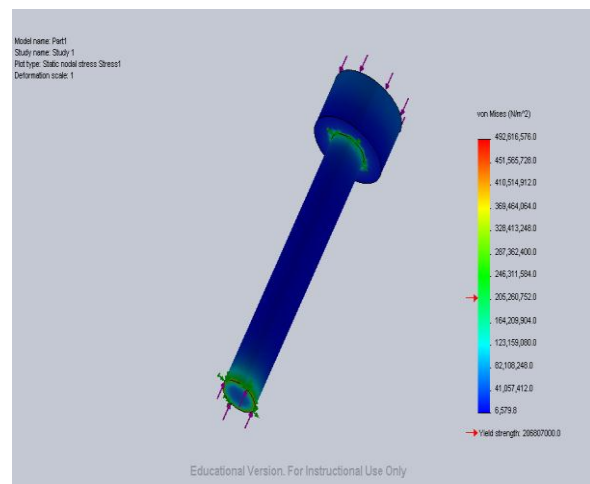


Figure A-1: Part1-Study 1-Stress-Stress.

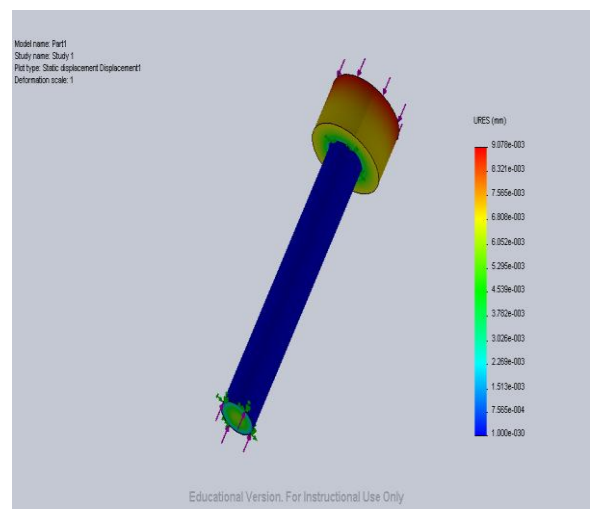


Figure A-2: Part1-Study 1-Displacement-Displacement.

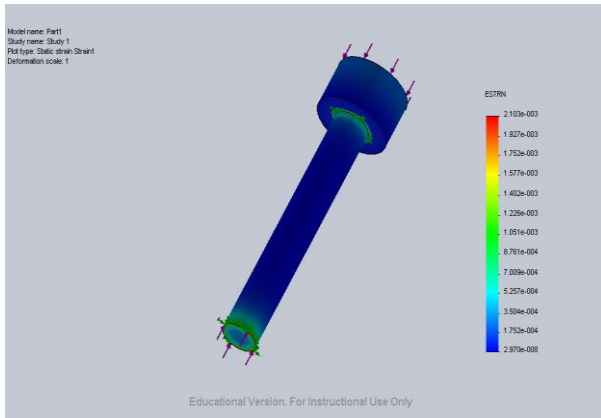


Figure A-3: Part1-Study 1-Strain-Strain.

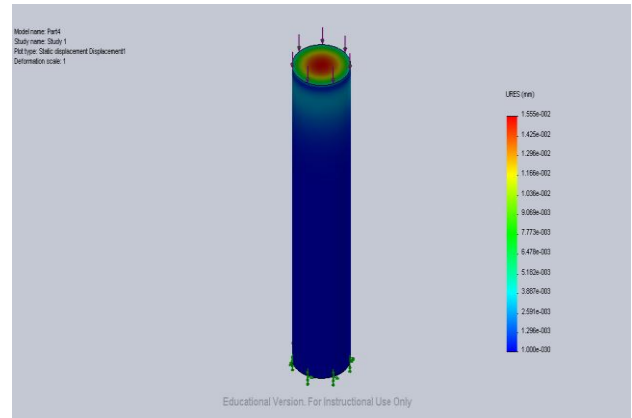


Figure A-5: Part4-Study 1-Displacement-Displacement.

2. Extruded work part

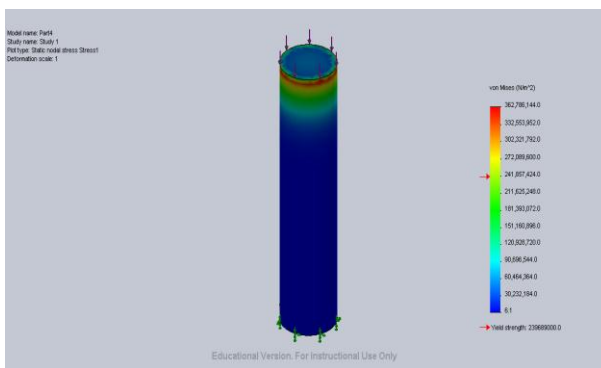


Figure A-4: Part4-Study 1-Stress-Stress.

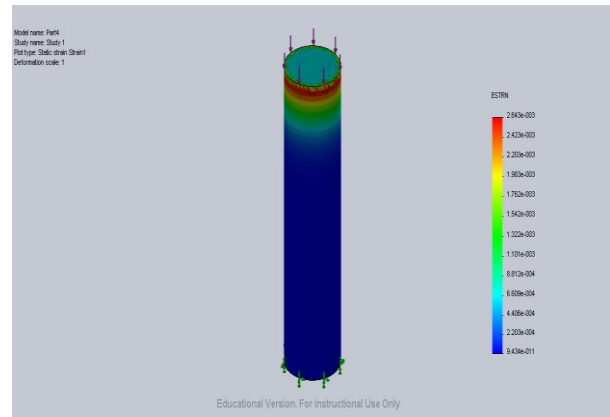


Figure A-6: Part4-Study 1-Strain-Strain.